Colloidal Stability for Concentrated Zirconia Aqueous Suspensions

Marie-Laure Rami,[‡] Martine Meireles,[†,§] Bernard Cabane,[¶] and Christian Guizard[‡]

[‡]Saint Gobain CREE/CNRS, Laboratoire de Synthèse et Fonctionnalisation des Céramiques, 84 306 Cavaillon, France

[§]Laboratoire de Génie Chimique, Universite De Toulouse, 31 062 Toulouse, France

[¶]Laboratoire de Physique et Mécanique des Milieux Hétérogène, ESPCI, 75231 Paris cedex 05, France

This work started as part of an investigation into the mechanisms by which fine zirconia aqueous dispersions can be processed for ceramic materials engineering. Aqueous dispersions of TZ3Y fine zirconia particles obtained by dispersion of dry powder in acidic solutions (pH 3) have been subjected to compression through osmotic experiments. The results show a behavior that is unusual when compared with the classical behavior of colloidal dispersions. Indeed, the 50 nm particles are well dispersed and protected from aggregation by electrical double layers, with a high zeta potential (60–80 mV). Yet, during osmotic compression, the dispersion goes from a liquid state to a gel state at a rather low volume fraction, $\phi = 0.2$, whereas the liquid–solid transition for repelling particles is expected to occur only at $\phi = 0.5$. This early transition to a state in which the dispersion does not flow may be a severe drawback in some uses of these dispersions, and thus it is important to understand its causes. A possible cause of this early aggregation is the presence of a population of very small particles, which are seen in osmotic stress experiments and in light scattering. We propose that aggregation could result from the compression of this population, through either of the following mechanisms: (a) An increase in pressure causes the small particles to aggregate with each other and with the larger ones or (b) An increase in pressure induces a depletion flocculation phenomenon, in which the large particles are pushed together by the smaller ones.

I. Introduction

The stability of concentrated colloidal dispersions is an important parameter for their processing in many industrial products. In ceramic engineering, materials with a high densification can be obtained by processing colloidal sols. Still, there are problems when interactions between particles are improperly controlled. In ceramic manufacturing, crack-free inorganic films, screen printing, or direct assembly techniques for instance require the processing of high solid content dispersions. Therefore, a growing number of studies are addressing the behavior of concentrated suspensions. Because of their large surface area and surface properties, submicrometer particles tend to form agglomerates that give rise to flaws in the final product, causing reductions in strength or reliability.[1]

Fine zirconia powder, especially doped with dissimilar oxides, has a high probability of aggregation, because of unavoidable hydratation reactions in aqueous solutions and an attractive Van der Waals force.[2] By carefully controlling the inter-particle forces, it might be possible to avoid or limit these aggregates. This is achieved by the introduction of a repulsive force into the system such that it outweighs the attractive force. In colloid chemistry, there are several methods of imparting stability to particles so that they do not aggregate. The first involves ionization on the particle surfaces. These surface groups, which can be negatively or positively charged depending on the pH, attract or repel counterions or co-ions in the solution to form an electrical double layer near the particles surface. The overlap of two electrical double layers leads to repulsions between particles and hence stabilization according to the DLVO theory.[3] However, when dispersed in pure water, yttrium-stabilized zirconia has an iso-electric point (IEP) near pH 8, which results in a very low surface charge under conditions of low ionic strength or else high ionic strength at pH values where the surface charge is high. In either case, the colloidal stability is expected to be limited. The second method of imparting stability is to adsorb polymers onto the particle surface.[4–6] This physically prevents the two particles from coming close enough to each other for the attractive force to dominate. When polymers on two particles overlap, there is a repulsive force due to osmotic pressure and elastic components. More recently a different route was proposed that consists in the addition of highly charged nanoparticles to nearly uncharged microspheres to prevent their natural aggregation.[7]

The aim of this paper is to examine the influence of an electrostatic stabilization on the behavior of concentrated aqueous zirconia dispersions. In the first step, we characterized the electrokinetic properties of the particles when dispersed in acidic solutions. Then we used osmotic compression measurements and rheological measurements to measure the efficiency of this protection when the dispersions are concentrated, i.e. the particles are brought close together. We determine the volume fractions where the system undergoes the liquid–gel and gel–solid transitions and compare them with those of the hard sphere system. This provides a view of the mechanisms by which dispersion is promoted and of mechanisms that control the stability when the dispersions are concentrated.

II. Experimental Procedure

(1) Materials

(A) Zirconia Powder: The source of yttria-doped zirconia was a well-characterized high-purity grade zirconia powder ZrO_2 doped with 3 mol% Y_2O_3 (Tosoh Manufacturing Co., TZ3Y Ltd, Tokyo, Japan). It has a BET surface area of 15 m^2/g and a density of 5.5 $g \cdot cm^3$. Examination of powder through transmission electron microscopy revealed that the primary particle size is around 50 nm. However, primary particles are organized in large aggregates with polydisperse sizes up to a few micrometers (Fig. 1). These aggregates are held together by very strong forces and do not spontaneously break up when they are dispersed in water.

Zirconia powder was dispersed in an aqueous acetic solution (CH_3COOH) or nitric solution (HNO_3). In some cases, pH or ionic strength was adjusted by NaOH or $NaNO_3$. These reagents were obtained from Aldrich (Saint Louis, MO). All preparations

G. Messing—contributing editor

Manuscript No. 24713. Received May 22, 2008; approved August 1, 2008.

Presented at the 10th International Conference on Ceramic Processing Science, May 25-28, 2008, Inuyama, Japan.

This work was financially supported by SAINT GOBAIN Recherches, Centre National de la Recherche Scientifique (CNRS-GDR 2980) and the National Research Agency (ANR CRUNCH).

[†]Author to whom correspondence should be addressed. meireles@chimie.ups-tlse.fr

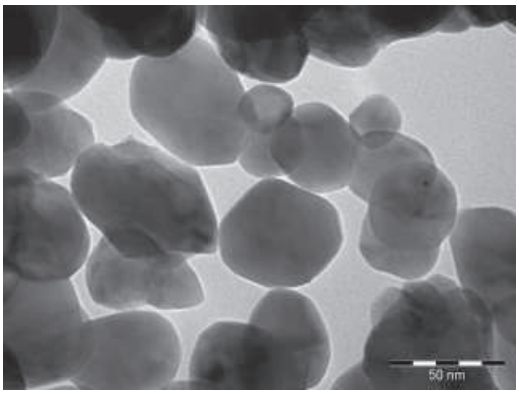

Fig. 1. Transmission electron microscopic (TEM) image of Tosoh TZ3Y powder.

were made with MilliQ® (Millipore Corp, Bedford, MA) water.

Dispersions were first stirred for an hour. Aggregate break-up was further promoted with an ultrasonic probe at 450 W for 120 s for a volume of 200 mL. With this procedure, suspensions containing up to 50% zirconia by weight (7% by volume) were prepared.

(2) Methods

(A) Electrokinetic Mobility: Electrophoretic mobility measurements were carried out using a Zetasizer3000 (Malvern) and converted to zeta potential. To check reproducibility, three samples were taken and six measurements were performed on each sample.

Measurements were made in diluted suspensions (solid content 0.05% zirconia by weight). Corrections for particle averaged dynamic mobility were performed using the software based the thin double-layer treatment.

(B) Particle Size Distribution: Particle size distribution was measured using a Zetasizer3000 (Malvern, Malvern Instruments, Worcestershire, U.K.). Measurements were made in dilute suspensions of solid content 0.05% zirconia by weight. Aliquots were prepared using the same solution as that used for the dispersion of the powder. Using this technique, we only characterize particles larger than 10 nm.

(C) Colloidal Stability: When using acetic or nitric solutions to disperse zirconia powder, specific ion adsorption on the surface of the particles may affect the colloidal stability. For most samples, colloidal stability could be easily determined visually, but assessment of the aggregation rate of the suspensions was preferred for better accuracy. To investigate the stability of the dispersions, we monitored the diameter of the dispersions over 90 min after sodium nitrate ($NaNO_3$) was added.

(D) Osmotic Compression: The application of a solution of high osmotic pressure on a dialysis bag containing a suspension of particles produces an osmotic stress on the suspension, which in turn induces the displacement of water molecules from the inside to the outside of the dialysis bag. This displacement of water molecules occurs naturally to counterbalance the difference in osmotic pressure taking place between the two compartments separated by the dialysis membrane. Using this process, it is expected that the suspension entrapped in the dialysis bag will be concentrated until an osmotic equilibrium is reached from both sides of the dialysis membrane.

For osmotic stress experiments, a volume of the dispersion (40 mL) was introduced in a dialysis bag (Spectra Por® Biotech membranes MWCO 15 000, Spectrum Laboratories, Rancho Dominguez, CA) and dialyzed against solutions of PEG 35000 at concentrations varying from 5 to 80 g/L prepared in the same acetic or nitric solutions as the dispersions. Dialysis was performed at room temperature (20°C). At the end of the dialysis, the concentrated dispersion of particles was collected from the dialysis bag and the solid content was measured using a thermogravimetric apparatus (Mettler Toledo, Viroflay, France). The final osmotic pressure was calculated from the final PEG concentration analyzed by TOC measurements. All preparations were made with MilliQ® water.

The osmotic pressure, Π, of PEG 35000 solutions can be represented by a polynomial function of the PEG concentration, c, in wt%[8]

For c (wt%) in the range $1 < c < 20$

$$\log \Pi = a + b[PEG]^c \quad (1)$$

with $a = 0.49$, $b = 2.5$, $c = 0.29$

According to this equation, the osmotic pressures applied in this work on the particle suspensions ranged from 0.5 to 400 kPa, using solutions containing 1–20 wt% of PEG.

(E) Rheology: Several rheological measurements were performed depending on the information required. In the first one, the measurements were made under small deformation such that the structure in the dispersion was not much disturbed from its equilibrium conditions (dynamic measurements). These measurements were informative for analyzing the structure of the system and the interactions between the particles. The second procedure involved measurements at a relatively large deformation, i.e. steady shear. The results were relevant for the system under flow conditions (steady-state measurements).

Steady shear and dynamic measurements were carried out using a Physica Anton Paar (MCR-300, Anton Paar GmbH, Graz, Austria)-controlled stress rheometer, with a smooth cone-plate geometry with a diameter of 50 mm and a cone angle of 1°. All measurements were carried out at 20°C. Samples were covered with oil to prevent evaporation.

Stress sweeps were conducted at an angular frequency of 0.1 s (0.6 Hz) to determine the rheological parameters as a function of the strain amplitude (0.01%–100%). This enabled us to obtain the viscoelastic region where the storage modulus G' and loss modulus G'' were independent of the applied strain. For steady-state measurements, shear stress versus shear rates were produced in a shear range between 10 and 2000 s^{-1} by increasing the shear rate in steps and then decreasing it. The measuring program was repeated twice for each sample to check reproducibility. Apparent viscosity data at a shear rate of 108 s^{-1} were used as the basis for comparing the different formulations.

(F) Redispersion: Some of the samples that were subjected to osmotic compression went through a sol–gel or a gel–solid transition. In order to assess the reversibility of these changes, redispersion experiments were performed. They consist in dispersing a known amount of concentrated samples in 20 mL (to reach a solid content of about 0.05% zirconia by weight). The particle size distribution was then measured to assess the size of aggregates remaining in the dispersion.

III. Results

(1) Electrokinetic Properties of Yttria-Doped Zirconia Powders

The ζ values of TZ3Y powder dispersed in nitric acid and acetic acid at various pH are given in Fig. 2. Also given are the zeta potential data for TZ3Y dispersed in water for pH adjusted with sodium hydroxide (NaOH) in the range 8–12. As expected, for TZ3Y zirconia powders dispersed in water,[9] the IEP value is in the pH range 7–8. The ζ values of TZ3Y powder dispersed in nitric acid are nearly constant in the pH range 3–6 and $= +45$ mV ($+/-5$ mV), whereas the ζ values of TZ3Y powder dispersed in acetic acid gradually increase for the same pH range, up to a value of +80 mV ($+/-5$ mV) at pH 3.

As no background electrolyte was added in these experiments, the molar concentration of ions for both systems can be easily deduced from the concentrations of acids or bases added to the solution. At pH 3, the molar concentrations of CH_3COO^- and NO_3^- are both equal to 0.001M. These count-

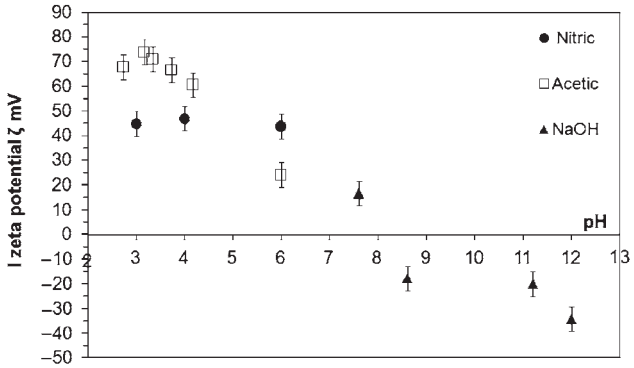

Fig. 2. Zeta potential versus pH for the TZ3Y powder in (filled squares) acetic acid, nitric acid (open circles), and sodium hydroxide (filled triangles).

erions are attracted to the particle surfaces and screen their surface charges. The behavior of the counterions near the surfaces also depends on their sizes: the size of CH_3COO^- is significantly larger than the size of NO_3^-. Because of this size difference, CH_3COO^- counterions may pack less densely in the Stern layer near the particle surfaces, compared with NO_3^-. Consequently, they may be less efficient at screening the surface charges, resulting in higher values for the measured electrokinetic potential.

(2) Particle Size Distribution

Experiments on the dispersion of dry alumina particle aqueous solutions have been discussed in previous works.[10] They demonstrate that the dispersion is controlled by a change in the balance of interparticle forces. In the dry powder, alumina particles are separated by thin films of adsorbed water and held together with Van der Waals forces. After immersion in water, repulsive forces (ionic pressure and hydration) cause redispersion if the net adhesion force becomes nearly zero. Based on the electrokinetic measurements presented above, we chose to disperse the powder at pH 3 where ζ values are at least equal to +40 mV for both acidic solutions.

The dispersion of the powder was monitored by PCS (Malvern Zetasizer 3000, Malvern Instruments, Worcestershire, U.K.). A fine particle size, close to the primary particle size of powder, is associated with a fully dispersed suspension. The results obtained for the dispersion of powder in nitric and acetic solutions show two populations: elementary particles (80 and 50 nm, respectively) and small aggregates (180 nm) probably composed of three to four primary particles (Fig. 3). Increasing the ultrasonic power or the time of irradiation caused a decrease in the efficiency due to an increase in the temperature. The results show a better efficiency when acetic solution is used for dispersion. This can be attributed to the large size of CH_3COO^- ions; when they condense near the particle surfaces, they form a more extended Stern layer compared with NO_3^- ions. The surfaces are then separated by a larger minimal distance, which is favorable for the redispersion.

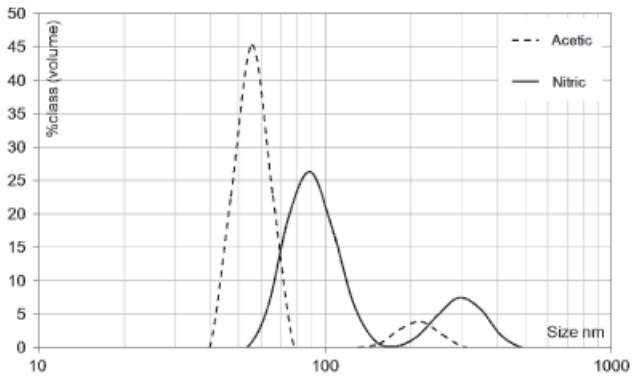

Fig. 3. Particle size distribution of TZ3Y (pH 3) dispersed in nitric acid and acetic acid with ultrasound.

(3) Colloidal Stability

To investigate the colloidal stability of dispersions, we monitored over 90 minutes the diameter of the dispersions after sodium nitrate ($NaNO_3$) was added.

In Fig. 4, we plotted the mean particle diameter given by PCS measurements (Zetasizer3000) as a function of time for TZ3Y powder dispersed in $0.001M$ acetic acid and for increasing concentrations of sodium nitrate $NaNO_3$. Assuming that the number of particles in the dispersion at a time t is related to the mean particle size according to

$$n_t = n_0 \left(\frac{a_t}{a_0}\right)^{1/D_f} \tag{1}$$

where n_t is the number of particles at t, n_0 is the initial number of particles, a is the mean size at t, a_0 is the mean size at $t = 0$, and D_f the fractal dimension of aggregate (approximated to 2), we determine the rate of aggregation k using the following equation:

$$k = \frac{\mathrm{d}\left(\frac{1}{n_t}\right)}{\mathrm{d}t} \tag{2}$$

Stability ratios W ($W = -\log(1/k)$) were then plotted in Fig. 5, for TZ3Y powder dispersed in nitric acid and acetic acid.

A minimal concentration of $0.01M$ of sodium nitrate $NaNO_3$ is required for reducing the repulsive barrier. After addition of sodium nitrate, the stability steeply decreases as a function of ionic strength in the range 0.01–$0.1M$. It then reaches a plateau (the stability no longer depends on ionic strength) above a critical coagulation concentration (CCC) of $0.025M$. (Note that the fractal dimension here does not impact the determination of the CCC). The experimental value of the CCC compares very well with the theoretical value of $0.022M$ for the CCC estimated from DLVO theory for the interactions between spheres of equivalent radii[11]

$$CCC = 3.9 \times 10^{-39} \frac{\gamma^4}{A^2 z^6} \text{ where } \gamma = \tan h\left(\frac{ze\zeta}{4k_B T}\right) \tag{3}$$

where ζ is the zeta potential (V); A is the Hamaker constant, $A = 7.23 \times 10^{-20}$ J for 3Y–ZrO_2; z is the ion valency; and e is the electronic charge (1.60×10^{-19} C).

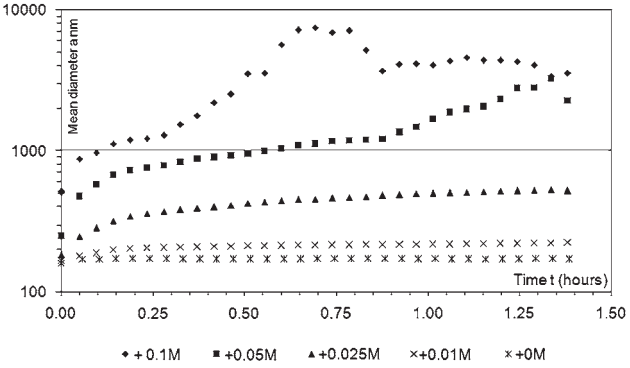

Fig. 4. Kinetics of aggregation for TZY powder dispersed in nitric acid: mean diameter measured by PCS versus time for increasing concentration of $NaNO_3$.

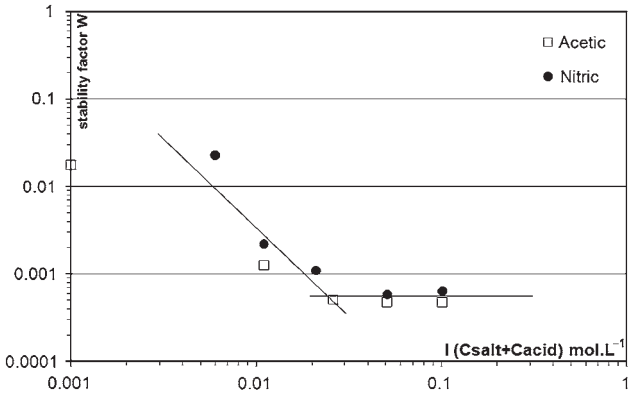

Fig. 5. Stability ratio for Tosoh TZ3Y dispersed in nitric (circles) and acetic (squares) acid solutions (pH 3). Ionic strength was adjusted by addition of $NaNO_3$.

(4) Osmotic Compression

Dispersions prepared in nitric and acetic acid have been dialyzed against PEG solutions as described in the previous section. The osmotic stress method was used to produce highly concentrated samples that could not be prepared by the ultrasonic method and also to better characterize the surface–surface interactions when the distance between the particles is reduced. Figure 6 gives a logarithmic representation of the osmotic pressure versus volume fraction (or surface–surface distance) for the two systems.

Three separate regimes can be clearly distinguished. At a low volume fraction (smaller than 0.10), the osmotic pressure increases with the solid content. Visual inspection of the samples in the dialysis bag indicates that the samples are still in the liquid phase. At an intermediate volume fraction in the range 0.18–0.45, a transition occurs toward a regime with a very small slope, almost forming a plateau. Visual inspection of the samples at this stage reveals that the system crossed the liquid–gel transition. The samples had an iridescent gel texture. At a high volume fraction (higher than 45%), a strong resistance to compression is present, leading to a large slope of the pressure versus volume fraction. At this point, visual inspection indicates that the system entered a solid paste domain. The samples had a noncohesive granular texture. Quantitative viscosimetric and viscoelastic measurements were carried out on liquid and gel-like samples. Results are presented in the next section. For samples obtained in the paste solid domain, standard rheological tests could not be performed.

Data points are not significantly different when different counterions are used. Therefore, the nature of the counterions does not seem to considerably influence the osmotic pressure of the dispersions of zirconia particles at least in the gel and the solid regime.

In order to further assess the contribution of electrostatic interactions to the osmotic pressure, the screening length was varied using a $0.01M$ ($NaNO_3$) concentration in the dialysis reservoir and in the dialysis bags. The value of the osmotic pressure was chosen to be well in the second regime within the apparent plateau. By reducing the screening length, the effectiveness of the potential barrier was decreased. Under such conditions, only two regimes were distinguished: the "liquid regime" and the "paste" regime.

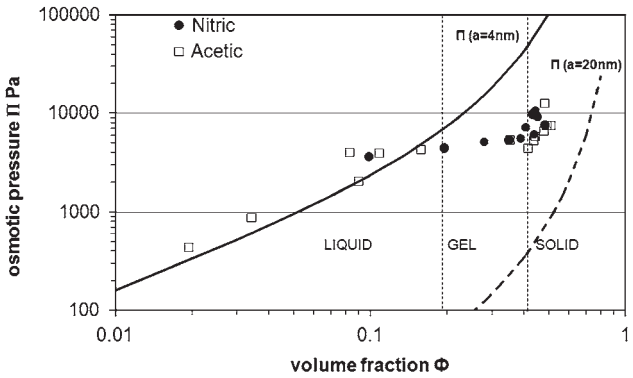

Fig. 6. Osmotic compressions of Tosoh TZ3Y powder dispersed in nitric (circles) or acetic solutions (squares). The vertical axis refers to the osmotic pressure measured after 7 days of equilibration pressure and the horizontal axis refers to the volume fraction. Continuous lines represent pressures calculated from Eq. (5) using different particle sizes.

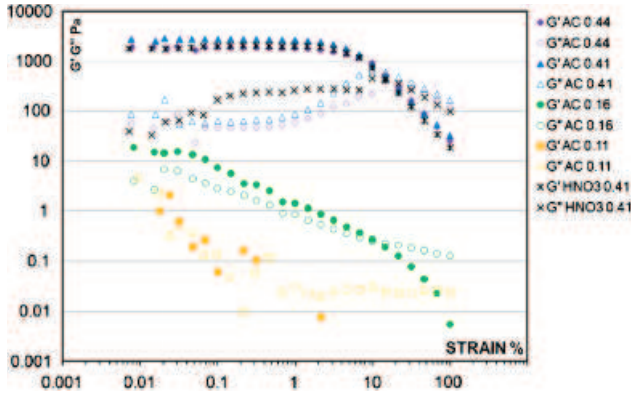

Fig. 7. Plots of elastic and loss modulus of compressed dispersions obtained in the liquid and gel (plateau regime) versus strain at a given frequency 0.6 Hz (AC refers to zirconia powder dispersed in acetic solution and HNO_3 to zirconia powder dispersed under nitric conditions).

(5) Viscoelastic Measurements

Figure 7 shows the storage and loss moduli (G', G'') as a function of strain amplitude at 0.6 Hz for concentrated acetic and nitric dispersions collected in the two different regimes: the "liquid" phase and the "gel" phase. For dispersions in the gel phase (volume fraction in the range 0.18–0.45), storage moduli in the range of 2000–3000 Pa are measured at low strains, transforming into a low liquid modulus at high strains. For dispersions in the liquid phase (volume fraction lower than 0.18), storage modulus was negligible. Again, data do not indicate a specific influence of the nature of the counterion on the structure of the dispersion in the gel regime.

(6) Viscosimetric Measurements

Steady-state flow curves obtained for dispersions up to a volume fraction of 0.10 show a Newtonian behavior and apparent viscosity was directly deduced from flow curves. For more concentrated samples, a shear thinning regime was observed. In these cases, apparent viscosity was determined for a given shear rate of 108 s^{-1}. Figure 8 shows the values of the apparent viscosity versus volume fraction for dispersions prepared with acetic acid. We noted the quantitative agreement between the results and the Krieger–Dougherty model for volume–fraction dependence of the viscosity of dense spheres.[3] Data were fitted with a maximum packing fraction $\phi_m = 0.2$ and $[\eta] = 5$.

(7) Redispersion

The redispersion of samples compressed in the plateau regime was followed by granulometric measurements for conditions where no salt was added. The results show a broader size distribution compared with the size distribution observed for initial dispersion (Fig. 9). Indeed, after osmotic stress, the distribution shows an increase in the proportion of aggregates in a size range of 300 nm. Still, only a fraction of primary aggregate particles were aggregated during compression, which indicates that under such conditions the repulsive potential barrier is effective.

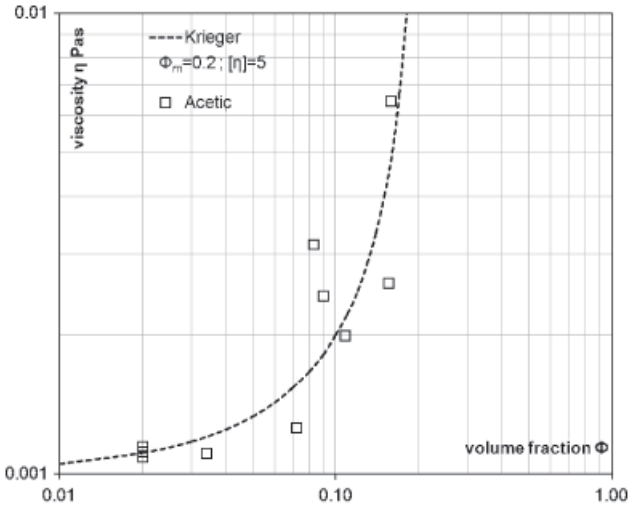

Fig. 8. Experimental data (filled squares) for the viscosity of dispersions as a function of volume fraction measured at a shear rate of $\gamma = 108\ s^{-1}$ for zirconia powder dispersed in acetic acid. Theoretical values (dashed line) of $\eta(\Phi)$ from the Krieger–Dougherty model fitted with $\Phi m = 0.2$ and $[\eta] = 5$.

IV. Discussion

The results presented above show a behavior that is unusual when compared with the classical behavior of colloidal dispersions. Indeed, the particles are well dispersed and protected from aggregation by electrical double layers, with a high zeta potential (60–80 mV). Yet, during osmotic compression, the dispersion goes from a liquid state to a gel state at a rather low volume fraction, $\phi = 0.2$, whereas the liquid–solid transition for repelling particles is expected to occur only at $\phi = 0.5$. This early transition to a state in which the dispersion does not flow may be a severe drawback in some uses of these dispersions and thus it is important to understand its causes. In the following discussion, we examine the successive stages of the compression of the dispersions, which are shown in Fig. 6: the liquid regime (up to $\phi = 0.2$), the liquid–gel transition, the gel range ($0.2 < \phi < 0.4$), and the paste range (beyond $\phi = 0.4$).

(1) The Liquid Regime

At low applied pressures (400–4000 Pa), the osmotic pressure and the volume fraction of zirconia are proportional to each other (Fig. 6). This is Van't Hoff's law for the osmotic pressure from noninteracting species. Accordingly, in this regime, the resistance to compression originates from species that are sufficiently dilute that they do not interact (perfect gas behavior). However, in this range of volume fractions, the pressure from the main population of zirconia particles (mean radius 50 nm) should be only 4–40 Pa, which is 100 times lower than the measured pressures. Therefore, the measured pressures must originate from other particles, much more numerous, and therefore necessarily much smaller than the zirconia particles in the main population. The number of these particles must be such that they produce high osmotic pressures, and their sizes must be such that they do not cross the dialysis membranes used in the osmotic stress experiments (otherwise, they would not contribute to the osmotic pressure). For instance, a population of particles with a mean radius of 2 nm and a volume fraction that would be 1/20 of that of the main population would produce the pressures that have been measured in the liquid regime.

Regarding the presence of very small nanoparticles, we may consider the solubility of the ZrO_2 under acidic conditions and elevated temperature. Its is well known that Zr^{4+} ions can peptize into larger species of 20–40 metal atoms with oxygen bridging. The experimental processing with ultrasonication may be a route to the formation of these types of species, which could be the source of the high osmotic pressures and zeta potential

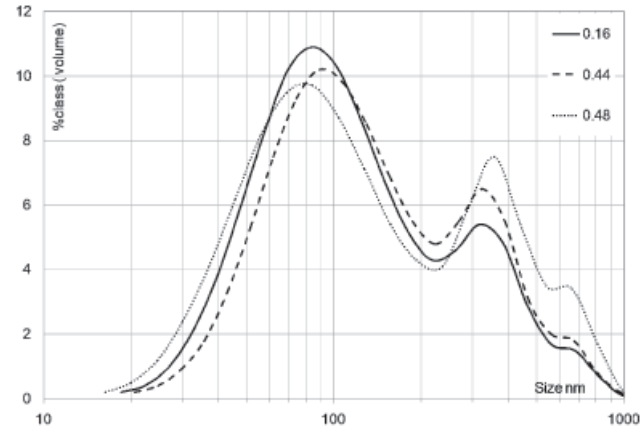

Fig. 9. Redispersion tests: particle size distribution of dispersion compressed in the plateau regime after redispersion in water.

values at the interfaces. We have attempted to characterize this population by physical separation of the large and small particles. Centrifugation at 3000 rpm for 1 h produces a supernatant that is completely clear. In quasielastic light scattering, the intensity of light scattered by this supernatant is three times that of water. The self-correlation function of the scattered intensity can be fitted with combinations of particle sizes that are in the 1–5 nm range. However, a more precise characterization of these small particles would require a small-angle X-ray or a neutron scattering experiment.

(2) The Gel State

When the applied pressure reaches 4000 Pa, the liquid dispersion becomes a gel. This transition is evident in mechanical measurements, because the dynamic measurements give a storage modulus that is higher than the viscous modulus (Fig. 7) and the steady shear viscosity diverges (Fig. 8). Yet, because the volume fraction is still rather low ($\phi = 0.2$), there is plenty of room for the particles to move about. If particles are unable to move, it must be that they are bound to each other, i.e. aggregated.

At first glance, it is surprising to find aggregation at such low volume fractions. Indeed, the ionization of the zirconia surfaces produces electrical double layers that must produce strong interparticle repulsions. We have calculated the free energy for a pair of particles according to the DLVO theory, for spherical particles with a diameter of 50 nm, with an electrical surface potential that is equal to the measured zeta potential (Fig. 10) and taking into account the Van der Waal attractions between particles, characterized by the Hamaker constant of zirconia, which is 17 kT^2.

This interaction free energy was calculated through Eq. (4):

$$G_{\mathrm{DLVO}} = G_{\mathrm{EDL}} + G_{\mathrm{VdW}} = 32\pi\varepsilon\left(\frac{kT}{ze}\right)^2 a\gamma_0^2 \exp(-\kappa h) - \frac{Aa}{12h} \tag{4}$$

where e is the dielectric constant of the liquid, kT the energy of thermal agitation, ze the electrical charge of the counterions, a the particle radius, h the separation between particle surfaces, k the Debye screening length, and γ_0 is a function that depends on the surface electrical potential ψ_0 of the particles according to

$$\gamma_0 = \tan h\left(\frac{ze\psi_0}{4kT}\right) \tag{5}$$

The variation of the interaction free energy with the separation of two particles is shown in Fig. 10. It is strongly attractive at very short distances, due to the very strong Van der Waals attractions between particles. But at large distances there is a strong repulsive barrier due to the overlap of the electrical dou-

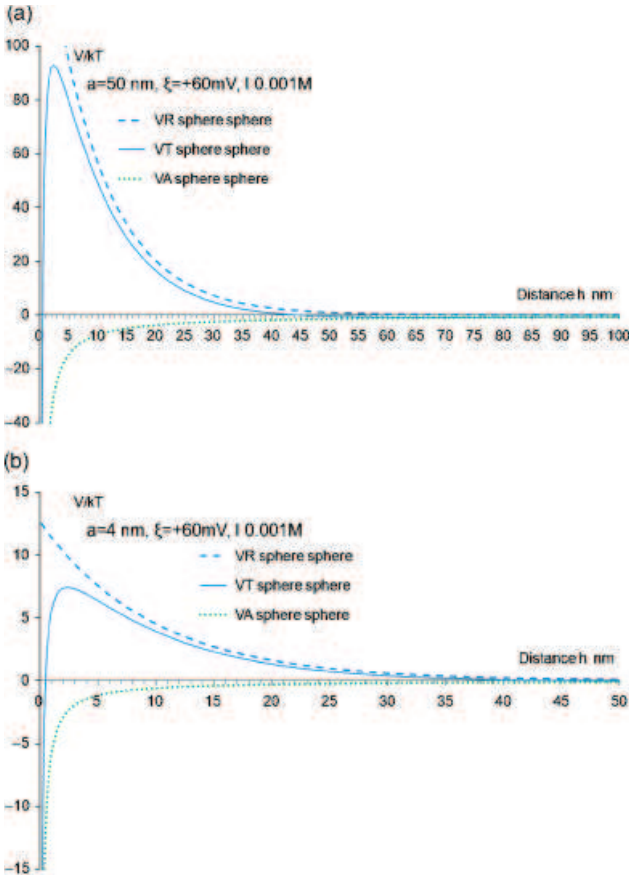

Fig. 10. (a) Free energy of interaction for a pair of large (50 nm) zirconia particles, calculated according to Eq. (4) with an electrical surface potential of 60 mV and a Hamaker constant equal to 17 kT. (b) Free energy of interaction for a pair of small (radius 4 nm) zirconia particles, calculated according to Eq. (4) with an electrical surface potential of 60 mV and a Hamaker constant equal to 17 kT.

ble layers. Because the height of this barrier is 75 kT, it should prevent particles from approaching each other and thus aggregation should not occur at volume fractions as low as $\phi = 0.2$, where the interparticle distances are on the order of 100 nm, well beyond the repulsive barrier.

On the other hand, aggregation could result from the compression of the small particles, through either of the following mechanisms.

(a) The increase in pressure causes the small particles to aggregate with each other and with the larger ones. Indeed, the electrical double-layer repulsions of very small particles are much smaller than those of the larger ones. We have calculated the interparticle pair interaction free energy of very small spherical particles with a diameter of 4 nm, and the same zeta potential and Hamaker constant as for the larger ones. The variation of this interaction free energy with the separation of two small particles is shown in Fig. 10. In this case, the height of the repulsive barrier is only 6 kT, which is not enough to prevent aggregation altogether. Similarly, the interaction free energy for a small particle interacting with a very large one (modeled as a half-plane) only has a weak repulsive barrier. The mechanism of aggregation would then be as follows: osmotic compression would increase the collision rate of small particles, to the point where aggregation proceeds slowly. The aggregates of small particles would then form a network that would trap the larger ones and prevent flow in the dispersion.

(b) The increase in pressure induces a depletion flocculation phenomenon, in which the large particles are pushed together by the smaller ones. This depletion flocculation mechanism is well known to occur in two-component systems such as latex dispersions containing excess water-soluble polymers[12] and emulsions containing excess surfactant.[13] Indeed, if the larger particles repel the smaller ones, the space between two larger particles is excluded to small particles. The free energy of the system is then lowered if the large particles are pushed together so that this excluded volume is reduced. The larger particles would then form loosely connected aggregates that would restrict flow in the dispersion. They would not be in the primary minimum of the DLVO interaction (this is still prevented by a very high (60 kT) barrier, but they would nevertheless be stuck to each other by an adhesive force that leads to the following adhesion free energy:[14]

$$G_{\text{depletion}} = -P\Delta^2.2pa \tag{6}$$

where P is the applied osmotic pressure, Δ the thickness of the layer around a large particle that is excluded to small ones, and a the radius of the large particle. With $P = 2000$ Pa, $\Delta = 10$ nm, and $a = 40$ nm, this yields $G_{\text{depletion}} = 12\,kT$, which is enough to produce aggregation.

These two mechanisms may have different consequences for the state of the dispersions. Mechanism (a) would produce permanent aggregates of the smaller particles, so that the concentrated dispersion would not redisperse spontaneously upon dilution. Mechanism (b) would not produce any permanent aggregates, and therefore the aggregates of large particles would redisperse spontaneously upon dilution. The results presented in Fig. 10 indicate that a substantial fraction of the large particles do redisperse upon dilution, but that some aggregates remain permanently. Hence, it may be that both mechanisms (a) and (b) take place in succession. A good way to distinguish between these mechanisms would be to provide some steric stabilization to all particles: then mechanism (a) would disappear while mechanism (b) would still operate.

(3) The Paste Regime

When the applied pressure reaches 10 000 Pa, the volume fraction remains blocked at about $\phi = 0.4$, and the dispersion becomes a granular solid: when it is subjected to mechanical stress, it responds with fractures instead of plastic flow. This behavior indicates that most particles are aggregated, and that the aggregates resist the forces exerted by compressive stress or by shear stress. Indeed, redispersion experiments indicate that a growing fraction of particles can no longer be redispersed by dilution alone, and therefore must be aggregated (Fig. 9). This may be an effect of the high volume fraction that has been reached in this state: because the particles have nonspherical shapes, it is possible that some of them have been forced to come into direct contact at an earlier stage ($\phi = 0.4$) than would be the case for spherical particles ($\phi = 0.64$ for a random packing of spheres).

V. Conclusion

This work started as a part of an investigation into the mechanisms by which fine TZ3Y zirconia aqueous dispersions can be processed for ceramic materials engineering. Generally, interparticle attractions due to very strong Van der Waals forces tend to induce spontaneous aggregation and stand in the way of the processing of submicrometer dispersions. The results obtained in this work show a behavior that is unusual when compared with the classical behavior of colloidal dispersions.

In dilute dispersions, the 50 nm particles are well dispersed and protected from aggregation by electrical double layers, with a high zeta potential (60–80 mV). Yet, during osmotic compression, the dispersion goes from a liquid state to a gel state at a rather low volume fraction, $\phi = 0.2$. At the same time, the osmotic pressure increases to values that are much higher than the pressures expected for a dispersion of 50 nm particles at these volume fractions. These high pressures must originate from a population of very small particles (diameters between 3 and 10 nm) that coexist with the larger ones. We propose that aggregation could result from the compression of this population, through either of the following mechanisms: (a) aggregation of small particles that have a low colloidal stability, and formation

of a network of aggregates that would block flow in the dispersion and (b) aggregation of large particles through a depletion attraction caused by the exclusion of small particles in their vicinity.

Regarding the presence of very small nanoparticles, we may consider the solubility of the ZrO_2 under acidic conditions and elevated temperature. It is well known that Zr^{4+} ions can peptize into larger species of 20–40 metal atoms with oxygen bridging. The experimental processing with ultrasonication may be a route to the formation of these types of species, which could be the source of the high osmotic pressures and zeta potential values at the interfaces. A precise characterization of these small particles would require small-angle X-ray or neutron scattering experiments. If this analysis is confirmed, it would favor processing methods in which only the main population of large particles is compressed and the small ones are evacuated.

References

[1]F. F. Lange, "Powder Processing Science and Technology for Increased Reliability," *J. Am. Ceram. Soc.*, **72**, 3–15 (1989).

[2]L. Bergström, "Hamaker Constants of Inorganic Materials," *Adv. Colloid. Interface Sci.*, **70**, 125–69 (1997).

[3]E. J. W Verwey, and J. T. G Overbeek eds. *Theory of the Stability of Lyophobic Colloids. The Interaction of Sol Particles Having an Electrical Double Layer*. Elsevier, Amsterdam, 1948.

[4]W. Huisman, T. Graule, and L. J. Gaukler, "Centrifugal Slip Casting of Zirconia," *J. Eur. Ceram. Soc.*, **13**, 33–9 (1994).

[5]P. C. Hidber, T. J. Graule, and L. J. Gauckler, "Influence of the Dispersant Structure on Properties of Electrostatically Stabilized Aqueous Alumina Suspensions," *J. Eur. Ceram. Soc.*, **17**, 239–49 (1997).

[6]P. C. Hidber, T. J. Graule, and L. J. Gauckler, "Citric Acid—A Dispersant for Aqueous Alumina Suspensions," *J. Am. Ceram. Soc.*, **79**, 1857–67 (1996).

[7]V. Tohver, J. E. Smay, A. Braem, P. V. Braun, and J. A. Lewis, "Nanoparticle Halos: A New Colloid Stabilization Mechanism," *Proc. Natl. Acad. Soc. USA*, **98** [16] 8950–4 (2001).

[8]A. Bouchoux, Personal communication, 2008.

[9]W. C. J. Wei, S. C. Wang, and F. Y. Ho, "Electronic Properties of Colloidal Zirconia Powders in Aqueous Suspension," *J. Am. Ceram. Soc.*, **82**, 3385–92 (1999).

[10]S. Desset, O. Spalla, and B. Cabane, "Redispersion of Alumina Particles in Water," *Langmuir*, **16**, 10495–508 (2000).

[11]R. F. Probstein (ed.) *Physicochemical Hydrodynamics: An Introduction*. Butterworths, Boston, 1989.

[12]P. R. Sperry, "A Simple Quantitative Model for the Volume Restriction Flocculation of Latex by Water-Soluble Polymers," *J. Colloid Interface Sci.*, **87** [2] 375–84 (1982).

[13]J. Bibette, F. Leal Calderon, V. Schmitt, and P. Poulin, *Emulsion Science*. Springer, Verlag, 2002.

[14]G. J. Fleer, M. A. Cohen Stuart, J. M. H. M. Scheutjens, and T. Cosgrove, *Polymers at Interfaces*. Chapman and Hall, London, 1993. □